Enforcement of nonhomogeneous Dirichlet boundary conditions in GFEM using preprocessed nodal coefficients on the boundary

André Rudnytskyj

Diego Amadeu F. Torres

Paulo de Tarso R. Mendonça

Clovis S. de Barcellos

a.rudnytskyj@gmail.com

diego.amadeu@gmail.com

mendonca@grante.ufsc.br

clovis.barcellos@ufsc.br

Group of Mechanical Analysis and Design, Department of Mechanical Engineering, Federal University of Santa Catarina - UFSC (1st, 3rd and 4th authors). Trindade, Florianópolis, 88040-900, Santa Catarina, Brazil

Department of Mechanical Engineering, Federal University of Technology of Paraná - UTFPR (2nd author). 3131 Pioneiros Avenue, Londrina, 86036-370, Paraná, Brazil

Abstract. *The Generalized Finite Element Method (GFEM) proposes augmentation of the approximation subspace by adding special functions which may reflect the known information about the boundary value problem and the input data. This work presents a procedure to enforce nonhomogeneous essential boundary conditions inspired on the fact that the solution of a linear boundary value problem can be decomposed into a sum of a homogeneous solution and a particular one. Pre-processed nodal coefficients are computed through the solution of local systems of algebraic equations built from the interpolation condition of the a priori known Dirichlet data, defining a non-null particular solution; such coefficients can be enforced through standard manipulation of the global system of algebraic equilibrium equations. A classic problem of two-dimensional linear elasticity is tested to investigate the procedure, comparing the performance of the conventional C^0-GFEM and the C^k-GFEM.*

Keywords: *Generalized Finite Element Method, two-dimensional elasticity, Dirichlet boundary conditions, higher-order approximations, convergence analysis.*

1 INTRODUCTION

The procedure of adding hierarchical refinements to a set of shape functions associated with finite elements, allows the construction of richer ansatz spaces to approximate solutions of partial differential equations. Such procedure has been widely studied and developed in the past two decades under various forms. In this context, it can be stated that Melenk & Babuška (1996) in their so called partition of unity finite element method (PUFEM), and Duarte & Oden (1995) in their meshless method hp clouds, presented the two most seminal scientific work on the partition of unity method (PUM), a method which has its origins in the landmark work of Babuška et al (1994, sub: 1992) and which was referred to as the generalized finite element method (GFEM) by Strouboulis et al. (2000 and 2001). A more detailed overview of the development and history of the GFEM can be found in the work of Babuška & Banerjee (2012). Perhaps the most important aspect to be highlighted here is the fact that the distinctive characteristic between the PUFEM and the hp clouds is the choice of the partition of unity (PoU) and/or enrichment functions (refinements added) (Duarte, 2012, and Babuška & Banerjee, 2012). The extended finite element method (XFEM) is also included in this context, since it is basically identical to the GFEM (Belytschko et al., 2009, and Fries & Belytschko, 2006), even though it has been mainly used in the context of crack propagation problems, firstly investigated in 1998-1999 by Belytschko & Black (1999).

1.1 GFEM features

In the GFEM, the PoU functions are extrinsically enriched by functions defined in global coordinates. Extrinsic enrichment is characterized by adding unknowns to the nodes, such that each additional unknown is associated with a new applied enrichment functions (see, for instance, Duarte et al., 2000, and Torres et al., 2011), recalling that specific enrichment functions can be used independently in specific regions of the domain, as in the h-p Cloud Method of Duarte & Oden (1996).

The present work has dealt only with polynomial[1] extrinsic enrichments up to the 6th degree, applied on triangular meshes to study a model problem - triangular elements allows the use of a consolidated integration technique. In the GFEM, a mesh of elements is created, as Torres et al. (2011) details, to facilitate the numerical integration, and define the PoU and geometry of the domain (reducing computational cost and simplifying the implementation in comparison to the h-p Cloud Method).

Consider a conventional finite element triangulation, $\{\mathcal{K}_e\}_{e=1}^{NE}$ (*NE* being the number of elements in $\mathcal{K}_e$), defined by *N* nodes with coordinates $\{\boldsymbol{x}_\alpha\}_{\alpha=1}^{N}$, for an open-bounded polyhedral domain $\Omega \subset \mathbb{R}^2$. For a node α, the cloud or patch ω_α is given by the union of finite elements sharing the node α of the FE mesh covering the domain of interest Ω. The set $\Im_N = \{\omega_\alpha\}_{\alpha=1}^{N}$, in a finite element mesh with N nodes, is an open cover of Ω, that is, the closure $\overline{\Omega}$ of the domain is contained in the union of the cloud closures $\overline{\omega}_\alpha$, such that $\overline{\Omega} \subset \bigcup_{\alpha=1}^{N} \overline{\omega}_\alpha$. In addition, according to Oden & Reddy (1976), a set of functions $\mathfrak{S}_N = \{\varphi_\alpha\}_{\alpha=1}^{N}$, each one being a *bump function* (every *bump function* has a compact support - see Torres' PhD Thesis, 2012 for more details) and having the corresponding cloud ω_α as its compact support, is called a Partition of

[1]Special enrichment functions may be used in this context to provide more accurate simulations, built on $a\ priori$ knowledge regarding the analytical expressions which could reflect the nature of the solution of a problem, like crack modeling (see Torres et al. (2015)).

Unity, subordinated to the covering $\Im_N$. In this work, the functions φ_α will be referred to as PoU. A PoU has the following properties: $\varphi_\alpha(\boldsymbol{x}) \in C_0^k(\omega_\alpha)$, with $k \geq 0$; $\Sigma_{\alpha=1}^N \varphi_\alpha(\boldsymbol{x}) = 1$, with $\forall\ \boldsymbol{x} \in \Omega$; and every compact subset of Ω intersects only a finite number of the supports of the $\varphi_\alpha(\boldsymbol{x})$. It should be noted that the standard finite element shape function may be used as a PoU with $C_0^0(\omega_\alpha)$ regularity and, thus, can be used for implementation in the GFEM as presented by Barros et al. (2004) and Torres et al. (2010).

The GFEM approximation capability can be described as follows: let a function u be defined over a domain Ω covered by a set $\Im_N$. Let $\widetilde{u}_\alpha^i$ be a local approximation of u which belongs to a local subspace $\mathcal{X}_\alpha(\omega_\alpha)$ defined over the cloud support ω_α, such that $\mathcal{X}_\alpha(\omega_\alpha) = \text{span}\{\mathcal{L}_{\alpha i}\}_{i\in\mathcal{J}(\alpha)}$, where $\mathcal{J}(\alpha)$, $\alpha = 1, 2, \ldots, N$, is the index set which refers to the enrichment functions associated with each node, $\mathcal{L}_{\alpha i}$ denotes an enrichment function i related to the node α and N is the number of nodes of the connected domain. So, basically, GFEM proposes that each subspace $\mathcal{X}_\alpha(\omega_\alpha)$ may be chosen in such a way that $\mathcal{L}_{\alpha i} \in \mathcal{X}_\alpha(\omega_\alpha)$ can closely approximate $u|_{\omega_\alpha}$ over the cloud ω_α, without compromising the conforming requirement.

The enrichment functions $\mathcal{L}_{\alpha i}$ are simply the functions to be extended through the operation of extension (Tu, 2008) increasing the approximation subspace. The PoU and the enriched PoU are used to build the following Galerkin approximation, $\widetilde{\boldsymbol{u}}(\boldsymbol{x})$, on which it is detailed how it relates to the 2D elasticity standard FEM:

$$\widetilde{\boldsymbol{u}}(\boldsymbol{x}) = \underbrace{\sum_{\alpha=1}^{N} \hat{\varphi}_\alpha(\boldsymbol{x}) \begin{Bmatrix} u_{x_\alpha} \\ u_{y_\alpha} \end{Bmatrix}}_{\substack{\text{conventional FEM approximation,} \\ \text{considering only a PoU function per node}}} + \underbrace{\sum_{\alpha=1}^{N} \hat{\varphi}_\alpha(\boldsymbol{x}) \sum_{i=1}^{q_\alpha} \hat{\mathcal{L}}_{\alpha i}(\boldsymbol{x}) \begin{Bmatrix} b_{\alpha i} \\ d_{\alpha i} \end{Bmatrix}}_{\text{enrichment}} \tag{1}$$

where u_{x_α} and u_{y_α} are the nodal coefficients associated with the PoU, while $b_{\alpha i}$ and $d_{\alpha i}$ are the nodal coefficients associated with the enriched PoU. The entity q_α is the number of enrichment functions of each node. The hat on $\varphi_\alpha(\boldsymbol{x})$ and $\mathcal{L}_{\alpha i}(\boldsymbol{x})$ indicate a diagonal array of each entity, to be consistent with the array notation of u_{x_α} and u_{y_α}.

A superscript $p = 1, 2, \ldots, 6$ can be added to $\mathcal{L}_{\alpha i}$ in order to specify the enrichment degree being used. For instance, in the case of $p = 2$ the set of enrichments is given by $\mathcal{L}_{\alpha i}^2(x, y) = \left\{\overline{x}_\alpha, \overline{y}_\alpha, \overline{x}_\alpha^2, \overline{x}_\alpha\overline{y}_\alpha, \overline{y}_\alpha^2\right\}$, with $i = 1, 2, \ldots, 5$ and $\overline{x}_\alpha := \frac{(x - x_\alpha)}{h_{\alpha_x}}$ where a translation and a scaling are performed (similar as done by Torres et al, 2011). The translation prevents issues related to the distance between the elements and the origin of the global coordinate system. For example, in the case $\overline{x}_\alpha := (x - x_\alpha)/h_{\alpha_x}$, the x-coordinate x_α of the node α is used for translation and the characteristic length h_{α_x} of its cloud, taken as the x-projection of the largest distance from the node $\boldsymbol{x}_\alpha$ to each of their cloud edges, is used for scaling (Duarte et al., 2000). The procedure of scaling the enrichment is important to create a dimensional equivalence between big and small elements[2], and therefore reducing round off errors in the computation of stiffness coefficients. It should be mentioned that this scaling does not cause any distortion effect, as generally happens for mapped FEM shape functions, since the denominator h_α itself does not impart a tensor characteristic to the enrichment functions definition. Several experiments by Torres et al. (2011) and Mendonça et al. (2011) have supported this conclusion. It is important to note that the enrichment functions are zero at the position of the node precisely because of the

[2]Here, dimensional equivalence refers to the fact that the values of the enrichment functions are always unitary at the most distant point at the boundary of each cloud.

translation, and thus, they do not contribute to the approximation of the solution at the position of the node, but improving approximation capabilities around it.

1.2 The C^k Generalized Finite Element Method

Torres (2012) and Torres et al. (2015) investigate the influences exerted by the regularity of discretizations specifically in two-dimensional crack modeling through enrichment procedures (GFEM/XFEM), comparing C^k-GFEM with the standard C^0-GFEM. These two versions basically differ in their regularity; C^0-GFEM is the conventional version in which C^0-FEM shape functions are considered as PoU, having $C_0^0(\omega_\alpha)$ continuity (as studied by Torres et al., 2011), such as tent functions over simplex triangles or bilinear Lagrangian functions for quadrangular elements. The use of higher-order continuity functions has not been extensively explored in the community, in contrast to the almost universal use of C^0 functions. The motivation for that study rests on the fact that enrichment patterns impart a variation on the convergence rates in linear elastic fracture mechanics (LEFM), as discussed by Laborde et al. (2005) and Béchet et al. (2005).

The C^k-GFEM is a special version of the GFEM which employs a smooth PoU; it was presented by Duarte et al. (2006) and applied in works such as Barcellos et al. (2009), Mendonça et al. (2011), and Mendonça et al. (2013). The idea is to build approximations with arbitrary regularity, maintaining all interesting features of the GFEM, as described in the previous section. This research employs the Shepard scheme, which uses *weighting functions*, $\mathcal{W}_\alpha : \mathbb{R}^2 \to \mathbb{R}$, with the cloud ω_α as their compact support. The Shepard PoU functions subordinated to the covering $\Im_N$ are defined as

$$\varphi_\alpha(\boldsymbol{x}) = \frac{\mathcal{W}_\alpha(\boldsymbol{x})}{\sum_{\beta(\boldsymbol{x})} \mathcal{W}_\beta(\boldsymbol{x})}, \text{ with } \beta(\boldsymbol{x}) \in \left\{\gamma \mid \mathcal{W}_\gamma(\boldsymbol{x}) \neq 0\right\}. \tag{2}$$

It should be noted that the regularity of the Shepard PoU functions relies only on the regularity of the weighting functions $\mathcal{W}_\alpha$. Barcellos et al. (2009) evaluate different edge functions in the composition of the nodal weighting functions showing that this procedure is simple and robust. It is important to recall that other types of PoU may be used in computational mechanics, but for the Shepard scheme there is no limitation for the overlapping of clouds and no restriction on the shape of clouds and its elements. In this work the weighting function $\mathcal{W}_\alpha$ for a convex cloud ω_α is simply defined as the product of all *cloud edge functions* $\varepsilon_{\alpha,j}(\xi_j)$ as $\mathcal{W}_\alpha(\boldsymbol{x}) := \prod_{j=1}^{M_\alpha} \varepsilon_{\alpha,j}(\xi_j)$, where M_α is the number of *cloud edge functions* associated with the cloud ω_α, defined in terms of the parametric coordinates ξ_j normal to each edge j (Duarte et al., 2006).

Edwards (1996) proposed using the following definition for this infinitely smooth cloud edge function $\varepsilon_{\alpha,j}$, for a edge j belonging to a cloud ω_α

$$\varepsilon_{\alpha,j}(\boldsymbol{x}) := \begin{cases} e^{-\xi_j^{-\gamma}} & , \text{ if } \xi_j > 0, \\ 0 & , \text{ otherwise} \end{cases} \tag{3}$$

where γ is a positive constant. The cloud edge function is a strictly positive function inside the cloud that vanishes, together with all its derivatives, towards an edge, rendering a $C_0^\infty(\omega_\alpha)$ weighting function. The parametric coordinate ξ_j is independent for each edge, in the sense that

there exists no inter-dependence between edges. Barcellos et al. (2009) show how to scale the several edge functions of a cloud in order to have all of them unitary at the cloud node, and with the same decaying rate β, in order to reduce mesh dependencies. Herein, the exponential edge functions are used with $\gamma = 0.3$ and $\beta = 0.6$.

The construction of the cloud edge functions to build the C^k PoU of a specific node is performed on all edges belonging to that node's cloud, i.e. for $j = 1, 2..., M_\alpha$. The procedure described in this section is applicable only for convex clouds. Nevertheless, the construction process of the continuous PoU is quite versatile and the generalization for arbitrary polygonal clouds was presented by Duarte et al. (2006) through the use of *boolean* products (Rvachev & Sheiko, 1995) to modify the cloud edge function.

Remark 1. When the PoU is built from polynomial FE shape functions, as in conventional C^0-GFEM, the system of linear algebraic equations resulting from the variational equilibrium equation under study using (1) is linearly dependent (Duarte et al., 2000). On the other hand, when the PoU is built as quotients of exponential functions, as in the C^k version, the resulting global stiffness matrix is positive definite if the boundary conditions imposed are sufficient to prevent rigid body motions. Besides, due to its construction nature, the presented C^k PoU has the drawback of being capable of reproducing only a constant function, as Schaback et al. (2006) state, while a conventional PoU of the standard GFEM (such as tent functions for triangular meshes) already has 1st-degree reproducibility by itself[3], for each displacement component. Following the notation established by Mendonça et al. (2011 and 2013), when the C^k PoU is extrinsically enriched with a polynomial set of degree p, the approximation functions form a basis for polynomials of degree $b = p$. In contrast, for C^0 PoU functions over simplex elements, the enriched basis can reproduce polynomials of degree $b = p + 1$.

Remark 2. It was noticed that a large number of integration points is required to compute the elementary stiffness matrices, due to the peaks and undulations in the C^k enriched basis. It is observed that this necessity is directly related to the amount of prescribed coefficients and not necessarily to the complexity of the boundary condition; the more expanded is the approximation space, the more expensive is the integration cost. Moreover, the use of a C^k PoU has also direct influence; recall that an elementary stiffness matrix has the form $K^e = \int_{\Omega_e} \mathbf{B}^{eT} C^d \mathbf{B}^e d\Omega_e$ where $\mathbf{B}^e$ is an elementary deformation matrix and thus contains derivatives of the approximation functions, i.e. derivatives of the C^k PoU and enriched C^k PoU. Since a study about numerical integration was not an aspect of concern herein, in order to reduce the integration errors to negligible levels, it was used the Wandzura's rule (Wandzura & Xiao, 2003) of integration with 175 points throughout this work. Previous evaluations about the necessary integration (see Barcellos et al., 2009 & Mendonça et al., 2011), show that about 35 triangular rule integration points is usually sufficient to obtain adequate integration in the element, for enrichment degrees up to 4.

2 ENFORCEMENT OF NONHOMOGENEOUS DIRICHLET BOUNDARY CONDITIONS

In this section, a procedure to compute an appropriate set of nodal coefficients for the enforcement of nonhomogeneous Dirichlet boundary conditions in strong-form is presented.

[3]It should be noted that the tent functions for triangles could not produce the rigid body rotation.

Firstly, it should be noted that the usual structure of the standard displacement-based FEM is preserved in the smooth version of GFEM. The entire C^k-GFEM formulation, enters the program structure encapsulated in a single routine, that computes the set of approximation functions values and its derivatives in the same fashion as for FEM functions, which are subsequently used to compute the element contributions.

Let $\mathscr{U}$ and $\mathscr{V} \in \mathcal{H}^1(\Omega)$ be *Hilbert* spaces of order 1, which are standard Sobolev spaces of square integrable functions whose first derivatives are also square integrable (in the sense of Lebesgue), on the domain Ω. Specifically, $\mathscr{U}$ is the space of kinematically admissible functions and $\mathscr{V}$ is the space kinematically admissible variations (difference between two kinematically admissible functions), conventionally defined (see Babuška et al., 2010, for instance).

The continuous variational problem (weak formulation) for the linear elastostatic problem is: *find a vector valued function* $\boldsymbol{u} \in \mathscr{U}(\Omega)$, where $\boldsymbol{u} = \{u_x, u_y\}^T$, *such that*

$$\mathscr{B}(\boldsymbol{u}, \boldsymbol{v}) = \mathscr{L}(\boldsymbol{v}), \quad \forall\, \boldsymbol{v} \in \mathscr{V} \tag{4}$$

considering the definition of *energy norm* $\| \bullet \|_{\mathscr{U}} := \sqrt{\frac{1}{2}\mathscr{B}(\bullet, \bullet)}$ to specifically state that $\mathscr{U}$ has finite energy, that is, $\mathscr{U} := \left\{ \boldsymbol{u}(\boldsymbol{x}),\ \boldsymbol{x} \in \Omega\ : \|\boldsymbol{u}\|_{\mathscr{U}} < \infty \right\}$.

Additionally, following Babuška et al. (2011), it is important to define

$$\mathscr{U}_0 := \left\{ \boldsymbol{u}(\boldsymbol{x}) \in \mathscr{U}\ : \boldsymbol{u}(\boldsymbol{x}) = \boldsymbol{0},\ \boldsymbol{x} \in \Gamma_D \right\} \quad \text{and} \quad \mathscr{U}_{\Gamma_D} := \left\{ \boldsymbol{u}(\boldsymbol{x}) \in \mathscr{U}\ : \boldsymbol{x} \in \Gamma_D \right\}. \tag{5}$$

After that, making the assumption that $\boldsymbol{g}(\boldsymbol{x}) \in \mathscr{U}_{\Gamma_D}$, it is possible to write

$$\mathscr{U}_g := \left\{ \boldsymbol{u}(\boldsymbol{x}) \in \mathscr{U}\ : \boldsymbol{u}(\boldsymbol{x}) = \boldsymbol{g}(\boldsymbol{x}),\ \boldsymbol{x} \in \Gamma_D \right\} \tag{6}$$

where Γ_D is the Dirichlet portion of the domain boundary $\partial\Omega$ and $\boldsymbol{g}(\boldsymbol{x})$ is a nonhomogeneous essential (or displacement) boundary condition.

The proposed methodology is based on the decomposition $\boldsymbol{u} = \overline{\boldsymbol{u}} + \boldsymbol{u}_0$ with $\boldsymbol{u}_0 \in \mathscr{U}_0$ and $\overline{\boldsymbol{u}} \in \mathscr{U}_g$ where it is assumed that $\overline{\boldsymbol{u}}$ is

$$\overline{\boldsymbol{u}}(\boldsymbol{x}) = \boldsymbol{g}(\boldsymbol{x}), \quad \text{for } \boldsymbol{x} \in \Gamma_D. \tag{7}$$

At this point, it should be noted that the solution $\boldsymbol{u} \in \mathscr{U}$ is independent of the manner in which $\boldsymbol{g}(\boldsymbol{x}),\ \boldsymbol{x} \in \Gamma_D$ is extended into $\overline{\boldsymbol{u}} \in \mathscr{U}$, and many such extensions exist (Babuška et al., 2010). Nevertheless a particular type of extension, now taking into account the discretization used, may affect distinctively the accuracy of the local response near the Dirichlet boundary.

From this observation and making use of the GFEM framework, in which all the involved approximation functions may be easily known at any point in the domain, this work aims to analyze an alternative procedure to incorporate Dirichlet data along the solution process. Herein, the approximation subspaces used in the discretized version of Eq. (4) could be specified as $\mathscr{U}_{h,b,k}$ and $\mathscr{V}_{h,b,k}$ for taking into account features of the approximation functions used, that are, the characteristic dimension of elements h, the polynomial degree b and the regularity k, but the notation will be simplified as $\mathscr{U}_h$ and $\mathscr{V}_h$ without loss of generality.

Then, the first step of the present methodology is building an approximation for the Dirichlet data $\boldsymbol{g}(\boldsymbol{x})$ for $\boldsymbol{x} \in \Gamma_D$ using the approximation functions from $\mathscr{U}_h \subset \mathscr{U}$. All the GFEM approximation functions may be computed at any point $\boldsymbol{x}$ along Γ_D and thus a representation $\widetilde{\boldsymbol{g}}$ for $\boldsymbol{g}$ can be obtained in a pre-processing step, as explained in the next section.

Consequently, similar to Eq. (7), the representation $\widetilde{\boldsymbol{g}}$ determines a $\widetilde{\overline{\boldsymbol{u}}}(\boldsymbol{x})$ for $\boldsymbol{x} \in \Gamma_D$, such that $\widetilde{\overline{\boldsymbol{u}}}(\boldsymbol{x}) \in \mathscr{U}_{h,g}$ (the discretized version of Eq. (6)). Thus, substituting $\widetilde{\boldsymbol{u}} = \widetilde{\overline{\boldsymbol{u}}} + \widetilde{\boldsymbol{u}}_0$ in Eq. (4), a discretized variational equation can be stated as *to find an approximation* $\widetilde{\boldsymbol{u}}_0 \in \mathscr{U}_{h,0}$ *such that*

$$\mathscr{B}\left(\widetilde{\boldsymbol{u}}_0, \widetilde{\boldsymbol{v}}\right) = \mathscr{L}\left(\widetilde{\boldsymbol{v}}\right) - \mathscr{B}\big(\widetilde{\overline{\boldsymbol{u}}}, \widetilde{\boldsymbol{v}}\big) \;\; \forall\, \widetilde{\boldsymbol{v}} \in \mathscr{V}_h \tag{8}$$

using the a priori known $\widetilde{\overline{\boldsymbol{u}}}$. It is worth noticing that $\widetilde{\overline{\boldsymbol{u}}}$ approaches $\overline{\boldsymbol{u}}$ as the space $\mathscr{U}_h$ is refined.

In summary, the proposed approach is based on the computation of an appropriate set of nodal coefficients for the approximation functions associated to the nodes on the Dirichlet boundary.

Since GFEM applies external enrichments in such a way that the coefficients associated with the PoU and the enriched PoU, for any degree p of polynomial enrichment functions, may be known *a priori* for any $\boldsymbol{x} \in \Gamma_D$, such preprocessed coefficients are computed in order to create, firstly, an interpolation of $\boldsymbol{g}(\boldsymbol{x})$ on $\mathscr{U}_{h,\Gamma_D}$ resulting in a $\widetilde{\boldsymbol{g}}(\boldsymbol{x})|\boldsymbol{x} \in \Gamma_D$ and, in the sequence, to use it for building an extension $\overline{\boldsymbol{u}} \in \mathscr{U}_{h,g}$ considering the localization provided by the PoU associated to the nodes on Γ_D. Thus, after the determination of those coefficients, the solution procedure runs conventionally, as to seek for $\widetilde{\boldsymbol{u}}_0 \in \mathscr{U}_{h,0} \subset \mathscr{U}_0$ as in Eq. (8).

The goal of this work is to present a study regarding the construction of $\widetilde{\boldsymbol{g}}(\boldsymbol{x})$ and its effects on the global solution. Therefore, the local and global accuracies are of concern, which means analyzing the quality of the local representation $\widetilde{\boldsymbol{g}}$ for different discretizations and parameters of solution and to study how it imparts the global approximation, considering local and global measures.

Remark 3. The numerical evaluations were performed using the standard test problem of plane elasticity, such that the bilinear form $\mathscr{B}(\bullet,\bullet)$ and the linear functional $\mathscr{L}(\bullet)$, that correspond to the elliptic partial differential equilibrium equation $\mathbf{L}^T\,\boldsymbol{\sigma}(\boldsymbol{u}) + \boldsymbol{b} = \mathbf{0}$ in Ω, are defined as $\mathscr{B}(\widetilde{\boldsymbol{u}}, \widetilde{\boldsymbol{v}}) := \int_\Omega \boldsymbol{\varepsilon}^T(\widetilde{\boldsymbol{v}})\,\boldsymbol{\sigma}(\widetilde{\boldsymbol{u}})\,l_z\,d\Omega$ and $\mathscr{L}(\widetilde{\boldsymbol{v}}) := \int_\Omega \widetilde{\boldsymbol{v}}^T\,\boldsymbol{b}\,l_z\,d\Omega + \int_{\Gamma_N} \widetilde{\boldsymbol{v}}^T\,\overline{\boldsymbol{t}}\,l_z\,ds$, where l_z is the thickness of the body, assumed here to be a constant; $\boldsymbol{b} = \{b_x, b_y\}^T$ (the superscript T indicates transpose) are body force components and $\boldsymbol{t} = \{t_x, t_y\}^T$, $\boldsymbol{t} = \boldsymbol{n}\,\boldsymbol{\sigma}(\boldsymbol{u}) = \overline{\boldsymbol{t}}$ on Γ_N is the surface traction. The stresses, $\boldsymbol{\sigma} = \{\sigma_x, \sigma_y, \tau_{xy}\}^T$, are related to the strains, $\boldsymbol{\varepsilon} = \{\varepsilon_x, \varepsilon_y, \gamma_{xy}\}^T$, through the linear elastic relation $\boldsymbol{\sigma}(\boldsymbol{u}) = \mathbb{C}\,\boldsymbol{\varepsilon}(\boldsymbol{u})$, where $\mathbb{C}$ is a constitutive matrix. The strains are related to the displacements by $\boldsymbol{\varepsilon}(\boldsymbol{u}) = \mathbf{L}\boldsymbol{u}$, where $\mathbf{L}$ is the differential operator:

$$\mathbf{L} = \begin{bmatrix} \frac{\partial}{\partial x} & 0 \\ 0 & \frac{\partial}{\partial y} \\ \frac{\partial}{\partial y} & \frac{\partial}{\partial x} \end{bmatrix} \quad \& \quad \boldsymbol{n} = \begin{bmatrix} n_x & 0 & n_y \\ 0 & n_y & n_x \end{bmatrix}. \tag{9}$$

2.1 Determination of boundary coefficients

In order to approximate the prescribed displacement function $\boldsymbol{g}$ along the Dirichlet boundary Γ_D, a linear combination of the basis functions in $\mathscr{U}_h$ associated with the nodes on Γ_D is performed and an interpolation condition is imposed.

Let us consider, for instance, two consecutive nodes α and β with coordinates $\boldsymbol{x}_\alpha$ and $\boldsymbol{x}_\beta$, respectively, located on a boundary segment of Γ_D parallel to the global x axis[4], as shown in

[4]When working with polynomial enrichments, if the segment on Γ_D is parallel to a global axis (**x** or **y**), the en-

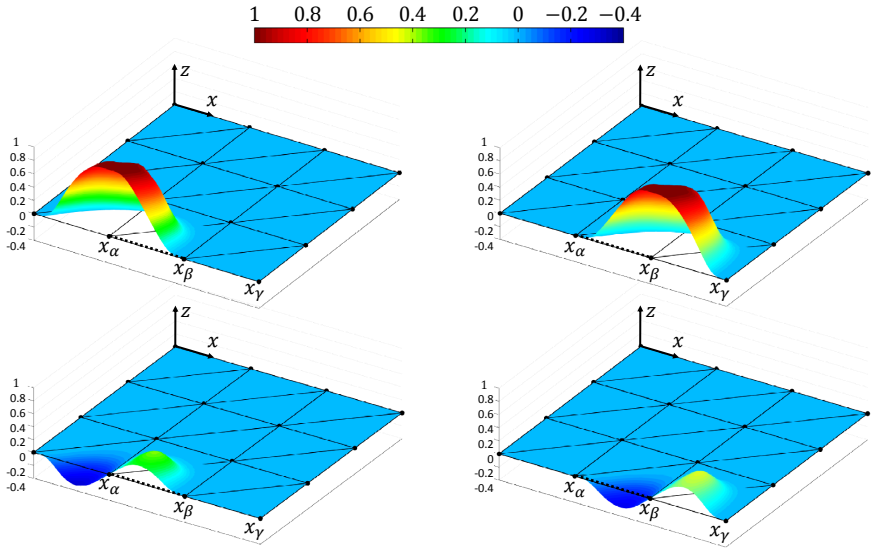

Figure 1: Illustrative mesh showing approximation functions associated with nodes α and β for $p = 1$; on the left, φ_α (top) and $\overline{x}\varphi_\alpha$ (bottom); on the right, φ_β (top) and $\overline{x}\varphi_\beta$ (bottom). The approximation along the segment between those two nodes is given by the linear combination of these functions.

Figure 1. For these nodes, the local approximation is spanned by the C^k PoU functions and polynomial enrichments of degree one, $p = 1$, and therefore $b = 1$ ((see **Remark 1**, end of section 1.2). Thus, the trace of the basis functions for such approximation along the boundary segment between these two nodes is composed by the following four functions (as shown in Figure 1): $\varphi_\alpha \times \left\{1, \overline{x}_\alpha\right\}$ and $\varphi_\beta \times \left\{1, \overline{x}_\beta\right\}$. In a case which the segment on Γ_D is non-coincident with a global coordinate axis, the local approximation will be spanned by $\varphi_\alpha \times \left\{1, \overline{x}_\alpha, \overline{y}_\alpha\right\}$ and $\varphi_\beta \times \left\{1, \overline{x}_\beta, \overline{y}_\beta\right\}$. Noticeably, a Galerkin approximation for the x-displacement component, for any point $\boldsymbol{x} \in \Gamma_D$, between nodes α and β, denoted by $\widetilde{\overline{\boldsymbol{u}}}_x(\boldsymbol{x})$, is obtained through the linear combination of those functions as:

$$\widetilde{\overline{\boldsymbol{u}}}_x(\boldsymbol{x}) = u_{x_\alpha}\varphi_\alpha(\boldsymbol{x}) + b_{\alpha 1}\,\overline{x}_\alpha\varphi_\alpha(\boldsymbol{x}) + b_{\alpha 2}\,\overline{y}_\alpha\varphi_\alpha(\boldsymbol{x}) + u_{x_\beta}\varphi_\beta(\boldsymbol{x}) + b_{\beta 1}\,\overline{x}_\beta\varphi_\beta(\boldsymbol{x}) + b_{\beta 2}\,\overline{y}_\beta\varphi_\beta(\boldsymbol{x}) \tag{10}$$

where the coefficients (see definition in Eq. (1)) are computed by imposing the interpolation condition for a point of interest $\boldsymbol{x}$ on that segment. The values of the approximation functions at such point of interest may be grouped in a 1×6 vector $\boldsymbol{\Phi}_{\alpha\beta}$, and the coefficients of the linear combination of Eq. (10) in a 6×1 vector $\mathbf{U}_{\widetilde{\overline{\boldsymbol{u}}}_x\alpha\beta}$. Therefore, the approximation of the x-displacement component on that point may be written as $\widetilde{\overline{\boldsymbol{u}}}_x(\boldsymbol{x}) = \boldsymbol{\Phi}_{\alpha\beta}(\boldsymbol{x})\,\mathbf{U}_{\widetilde{\overline{\boldsymbol{u}}}_x\alpha\beta}(\boldsymbol{x})$, recalling that $\widetilde{\overline{\boldsymbol{u}}}$, which is assumed to be punctually equal to $\widetilde{\boldsymbol{g}}(\boldsymbol{x})$, is known.

Hence, inspired by the Galerkin expansion, it is possible to select a sufficient number of points $\boldsymbol{x}$ along the boundary segment to build a linear system of equations in order to compute an appropriate set of coefficients.

richment functions in terms of the orthogonal coordinate will be null there. In that case, the coefficients associated with those functions are left free, in the sense that they will be computed only in the global problem of equilibrium. Thus, these functions may contribute to the solution inside the cloud, where such functions are non-null.

In fact, two procedures to build such systems of equations for the computation of the coefficients along Γ_D are presented in sequence. The first method, named *element-wise method*, involves the solution of two linear systems in order to find the coefficients for one node. Thus, considering C^k PoU and that the nodes of Figure 1 are enriched with monomials of degree one, so $b = 1$, and assuming the segment on Γ_D they belong to is non-coincident with a global coordinate axis, we build and resolve a system of equations such as Eq. (10) between nodes α and β selecting 6 evaluation points (for C^k PoU and $b = 1$, there are three unknowns for each node, i.e., six coefficients associated with the available approximation functions, where the nonhomogeneous boundary condition is evaluated). Consider, for simplicity of exposition, the displacement only in the x-direction.

$$\left[\ \mathcal{B}|_{\alpha\beta,6\times6} \ \right] \left[\ \mathbf{U}_{\widetilde{\overline{\boldsymbol{u}}}_x\alpha\beta,6\times1} \ \right] = \left[\ \mathcal{U}|_{\alpha\beta,6\times1} \ \right]. \tag{11}$$

Note that $\mathcal{B}|_{\alpha\beta,6\times6}$ is a 6×6 matrix, each row being a 1×6 vector $\mathbf{\Phi}_{\alpha\beta}$ evaluated at a point in the segment. The unknown 1×6 vector $\mathbf{U}_{\overline{u}_x\alpha\beta}$ contains the coefficients and $\mathcal{U}|_{\alpha\beta,6}$ is a 1×6 vector with each row being a $\widetilde{\overline{\boldsymbol{u}}}_x(\boldsymbol{x})$ evaluated at a point in the segment. Next, other 6 points are evaluated in the edge between nodes β and γ (Figure 1), analogous to system 11:

$$\left[\ \mathcal{B}|_{\beta\gamma,6\times6} \ \right] \left[\ \mathbf{U}_{\widetilde{\overline{\boldsymbol{u}}}_x\beta\gamma,6\times1} \ \right] = \left[\ \mathcal{U}|_{\beta\gamma,6\times1} \ \right]. \tag{12}$$

The node in which we are interested in the construction of (11) and (12) is node β. It is evident that solving them, two values for each one of the coefficients $u_{x\beta}$, $b_{\beta1}$ and $b_{\beta2}$ of node β are obtained. The fact is that the PoU of the central node β has the two adjacent elements as its support. It has been numerically observed that when the prescribed displacement function is smooth and the enrichment degree is not too high ($b \leq 3$), the two values for each coefficient of node β are practically the same. In other cases, the systems may become ill-conditioned and, therefore, the coefficients solution is less accurate. The simplest procedure consists in making an arithmetic average with both coefficients. If one wishes a better approximation on one side of the node, one shall use the coefficient related to that side. However, since we are looking for a good approximation of the displacement on the Dirichlet boundary as whole, it is better not to favor one side over the other.

The second possible procedure, called *cloud-wise method*, demands solving only one system per node; the two systems described in the element-wise method are coupled together to form one larger system (13), resulting in only one value for each coefficient of the node β:

$$\begin{bmatrix} \mathcal{B}|_{\alpha\beta,6\times6} & 0_{6\times3} \\ 0_{6\times3} & \mathcal{B}|_{\beta\gamma,6\times6} \end{bmatrix} \left[\ \mathbf{U}_{\widetilde{\overline{\boldsymbol{u}}}_x\alpha\beta\gamma,9\times1} \ \right] = \left[\ \mathcal{U}|_{\alpha\beta\gamma,12} \ \right]. \tag{13}$$

It is important to highlight the structure of the first matrix; in the case, its size is 12×9 because there are 3 approximation functions for each node, α, β and γ (see Figure 1). Columns 4 to 6 are all non-zero, containing the last 3 columns of the entity $\mathcal{B}|_{\alpha\beta,6}$ in the first 6 rows, and the first 3 columns of the entity $\mathcal{B}|_{\beta\gamma,6}$ in the last 6 rows. The number of rows equals the number of evaluation points[5] and the number of columns equals the number of functions. In this case, a definitive set of coefficients for node β is obtained.

[5]It is used the same number of points as in each segment of the element-wise method, in order to coherently compare both methods in the upcoming sections.

The entity $\mathbf{U}_{\widetilde{\overline{\boldsymbol{u}}}_x}$ in both methods provide the coefficients of the approximation functions of one specific node on the Dirichlet boundary (in the case, node β) and so, the selected procedure must be repeated for every element edge (or cloud) until all coefficients of all nodes on the Dirichlet boundary are determined. Note that these techniques may be applied regardless of the orientations of the segments along Γ_D boundary.

One may predict that there may be situations in which coefficients will need to be determined using only one system of the element-wise method. Cases such as the node γ showed in Figure 1, which is a node with only one edge of its support on the Γ_D; in that case, the coefficients of the node γ will be given by $\mathcal{V}|_{\beta\gamma,6}$ which is obtained from (12). Another example are nodes whose edges have different orientations and one of them matches a global axis, which means that some of its functions will be non-null on only one of the sides.

Once all the coefficients to all nodes on Γ_D are calculated, the GFEM runs conventionally until the solution of the global problem $\mathbb{K} \times \mathbb{U} = \mathbb{F}$, which results from the discretized formulation, noting that the vector $\mathbb{F}$ is substituted by a vector $\mathbb{F}' = \mathbb{F} - \mathbb{F}_u$ where $\mathbb{F}_u$ expresses the effects of $\widetilde{\boldsymbol{g}}(\boldsymbol{x})$, and the matrix $\mathbb{K}$ is also modified, conventionally.

2.2 Solving the Linear Systems

Before presenting results and a convergence study it is important to clarify some features and procedures in the solution of the linear systems. It is well known that when working with numerical analysis, one may eventually deal with matrices that present a large condition number. Mainly in higher-order methods, a condition number is a property of the matrix, or the linear system it represents and, therefore, independent of the algorithm employed to solve the system. A large condition number can be associated with a solution potentially in error (see Cheney & Kincaid, 2007).

Strouboulis, Babuška and colleagues (2000) have proposed an approach described by Duarte, Babuška & Oden (2000) to deal with linear dependencies originated due to the nature of the approximation functions in the conventional C^0 GFEM. In such case, the linear dependence is due to the fact that both the PoU and the basis of the local spaces $\mathcal{X}_\alpha$ are polynomial functions.

They propose to solve the systems of equations $\mathbb{K} \times \mathbb{U} = \mathbb{F}$, where the stiffness $\mathbb{K}$ is a positive semi-definite matrix, by transforming such matrix through a positive shifting in its main diagonal with a factor ϵ, turning it into a positive definite and hence non-singular. A iterative procedure follows according to a settled tolerance parameter. This approach will be referred to as *Babuška method* in the upcoming sections.

Duarte et al. (2000) comment that numerical experiments performed by Strouboulis et al. (2000) show that, in practice, using $\epsilon = 10^{-10}$ for the global equilibrium problem $\mathbb{K} \times \mathbb{U} = \mathbb{F}$, a single iteration is sufficient when using double precision accuracy. Each iteration involves a matrix-vector multiplication, a forward- and back-substitutions and lower order operations.

In contrast, the C^k-GFEM does not suffer from such a linear dependence in its stiffness matrix since the PoU functions and the enrichments have different algebraic nature. However, the Babuška method has been also used for the smooth version by Mendonça et al. (2011 and 2013) due to reasons that were discussed in Torres et al. (2015).

The Babuška method was employed to solve not only the global system $\mathbb{K} \times \mathbb{U} = \mathbb{F}$, but also the local linear systems to find the Γ_D boundary coefficients, as previously explained.

Besides, although the PoU of the C^k-GFEM is not a polynomial function, the local systems have more linear dependencies than one would expected[6]. Afterwards, it was observed that the local systems such as the one from equation (13) had rank deficiency and is not symmetrical. Hence, the least square method (LSM) needed to be employed at this point.

Least Square Method

The LSM was used to transform the matrices before employing the algorithm of Babuška. Consider, for instance, a generic linear system: $\mathbf{BV} = \mathbf{U}$, which is analogous to a system such as (11), (12), or (13). The goal is to find $\mathbf{V}$ through the quadratic minimization $\hat{\mathbf{V}} = \arg\min S(\mathbf{V})$, where S is given by

$$S(\mathbf{V}) = \sum_{i=1}^{m} |U_i - \sum_{j=1}^{n} B_{ij}V_j|^2 = ||\mathbf{U} - \mathbf{BV}||^2. \tag{14}$$

The solution of the minimization problem above, given by solving the normal equations, is

$$B^T B\hat{V} = B^T U. \tag{15}$$

Therefore, system (15) is the one to be resolved using the algorithm of Babuška. The LSM is used to overcome rank deficiency, but besides that, it also avoids non-positive numbers in the main diagonal of the matrix (systems (11), (12) and (13)), which would compromise the Jacobi pre-conditioning that Duarte et al. (2000) proposed to use along with the iterative method. The use of the LSM also allowed the symmetrization of the matrices, even for that from the cloud-wise method (see (13)) which is originally rectangular.

Hence, instead of solving systems (11) and (12), when using the element-wise method, and system (13), when using the cloud-wise method, we transform them using the LSM to obtain systems such as system (14); the resultant systems, which are system (15)-like, are named *local systems*.

One may notice that the algorithm of Babuška is employed several times, as many as are the number of local systems built to calculate all coefficients of all nodes on the Dirichlet boundary. At this point, the procedure used for the determination of the coefficients is complete and the rest of the general algorithm remains unchanged until the definition of the global system $\mathbb{K} \times \mathbb{U} = \mathbb{F}$, where the imposition of the coefficients could finally be performed.

3 MODEL PROBLEM - TWO DIMENSIONAL LINEAR ELASTICITY

A classic L-shaped domain, in the context of two dimensional linear elasticity, was the model problem employed to input the method and perform simulations. The analytical solutions for the displacement components of this problem are given by equations (16) and (17), according to Szabó & Babuška (2011)

$$u_x = \frac{A_1}{2G} r^{\lambda_1}[(\kappa - Q_1(\lambda_1 + 1))\cos\lambda_1\theta - \lambda_1\cos(\lambda_1 - 2)\theta] \tag{16}$$

$$u_y = \frac{A_1}{2G} r^{\lambda_1}[(\kappa + Q_1(\lambda_1 + 1))\sin\lambda_1\theta + \lambda_1\sin(\lambda_1 - 2)\theta] \tag{17}$$

[6]The orientation of the Dirichlet boundary can be such that the enrichment polynomials in the x and y direction provide equal (or opposite) function values of approximation. Hence, the orientation of the Dirichlet boundary defines if the system will become linearly dependent or not.

where r and θ are polar coordinates, $\lambda_1 = 0.544483737, Q_1 = 0.543075579$ and A_1 is considered 1. Additionally, the material properties considered are the Young modulus $E = 1000MPa$, the Poisson's ratio $\nu = 0.3$ and κ is a constant that depends only on the modulus of Poisson's ratio, which is $\dfrac{3-\nu}{1+\nu}$, for plane stress, and $3-4\nu$, for plane strain. $G = \dfrac{E}{2(1+\nu)}$ is the Coulomb modulus.

Herein, it was supposed the plane strain case. Three different meshes (Figure 2) containing only convex clouds were used to investigate *h*-refinement effects. The nonhomogeneous Dirichlet boundary conditions were enforced, following equations (16) and (17), on the boundary portion indicated.

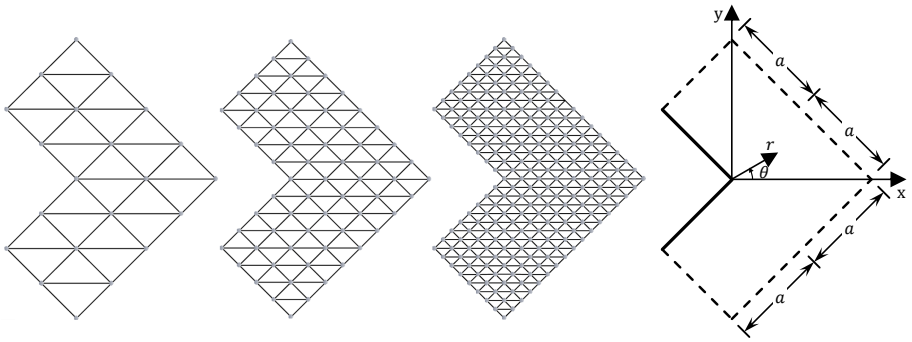

Figure 2: From left to right: meshes 1, 2, and 3 ,with 21, 65, and 225 nodes respectively. Origin of coordinate system and location of enforcement of Dirichlet boundary conditions indicated by dashed boundary.

The exact energy norm can be calculated as Barros et al. (2004) write

$$\|\boldsymbol{u}\|_E = 2.882549 \ \left((A_1)^2 \, a^{2\lambda_1} \, l_z/E\right)^{1/2}. \tag{18}$$

In the studied case, $a = 100$, which is the characteristic length (Figure 2), and $l_z = 1$, which is the constant and unitary thickness of the domain.

3.1 Perturbation & Tolerance

During the employment of the methodology of calculating Γ_D boundary coefficients in the model problem, it was observed that the main parameters of the Babuška method had considerable influence in the final result in terms of energy norm (Eq. 18). These parameters are the perturbation factor ϵ and the tolerance for the iterations.

The tolerance and the perturbation factor were fixed as 10^{-12} and $\epsilon = 10^{-10}$, respectively, when solving the algebraic system of equations for the discretized variational global equilibrium problem, as suggested by Duarte et al. (2000) in the context of GFEM. In the case of C^k PoU, the global stiffness matrix is theoretically not singular, and thus, it would not be necessary to use a perturbation, whose only purpose is to remove null-eigenvalues from the stiffness matrix. A more detailed discussion about conditioning in case of C^k-GFEM approximations is presented by Torres et al. (2015). Additionally, since stability is of concern in GFEM methodology, in general, it has been recently addressed, for example, by Babuška & Banerjee (2012), Gupta et al. (2012) and Sillem et al. (2015).

Nevertheless, when using the Babuška method (after applying the LSM for the local systems (11), (12) and (13)), it was observed that both parameters may have great influence on

the computation of the preprocessed coefficients for the nodes on the Dirichlet boundary. For this reason, a study was performed to identify the proper values for each parameter aiming to reduce the error in the computation of the boundary nodal preprocessed coefficients. This study allowed the setting of proper values for each parameter before verifying global convergence for the p and h refinement.

Various simulations were conducted and globally analyzed through the energy norm of the relative error in terms of the strain energy of the domain:

$$\|\boldsymbol{e}_r\|_E = \frac{\|\widetilde{\boldsymbol{u}} - \boldsymbol{u}\|_E}{\|\boldsymbol{u}\|_E} \tag{19}$$

recalling that $U(\bullet) = \dfrac{1}{2}\mathscr{B}(\bullet,\bullet) = \| \bullet \|_E^2$ is the strain energy of the exact solution (obtained through Eq. 18). It is important to highlight that $\|\widetilde{\boldsymbol{u}} - \boldsymbol{u}\|_E = \sqrt{U(\widetilde{\boldsymbol{u}}) - U(\boldsymbol{u})}$ as presented by Babuška & Suri (1987), page 220, equations (6.2) and (6.3).

The simulations allowed the construction of error surfaces (Figure 3) in which one can see the global error in terms of energy norm obtained when using several combination of the"local parameters", i.e., the perturbation factor ($pert^L$) and tolerance (tol^L) of the Babuška method used in the local systems. In fact, it was noticed that, regardless of the p degree, meshes or method to calculate the boundary coefficients, the error surfaces always presented the same characteristic shape. Figure 3 compares, for example, the two methods for mesh 1 (Figure 2) using $b = 2$.

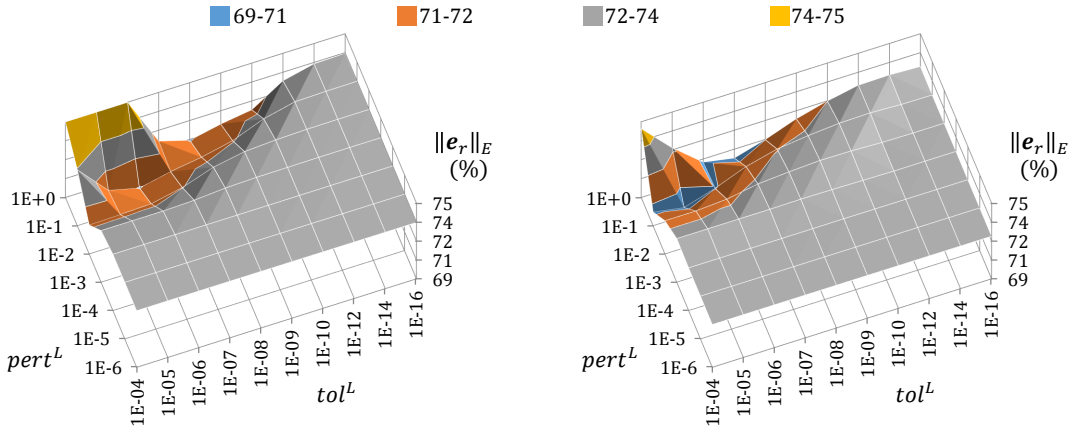

Figure 3: Global error surfaces in terms of energy norm for mesh 1, $b = 2$ for different combinations of the tolerance and perturbation of the coefficient's local systems; Element-wise method (left) and Cloud-wise method (right).

Figure 3 show that the local parameters may have a considerable influence in the global error (around 3 percentage points between average and lowest values), which justifies the importance of their study. It was also noted that the cloud-wise method provides, in general, slightly better results (in terms of the energy norm for the entire domain) compared to the element-wise method. As pointed out, for a higher p degree, the surface is basically shifted down to a lower error level, maintaining its shape. The finest results based on this global error measurement, have showed to be those for which the local perturbation factor is 10^{-0} or 10^{-1} and the local tolerance is 10^{-6}, 10^{-7} or 10^{-8}, for solving the local systems.

Simultaneously, the results were locally analyzed using the $\mathfrak{L}^2$-norm of the relative error in terms of the x-displacement on the Γ_D boundary:

$$\|\boldsymbol{e}_r\|_{\mathfrak{L}^2(\overline{u}_x,\Gamma_D)} = \frac{||\widetilde{\boldsymbol{u}}_x - \boldsymbol{u}_x||_{\mathfrak{L}^2(\Gamma_D)}}{||\boldsymbol{u}_x||_{\mathfrak{L}^2(\Gamma_D)}} \tag{20}$$

recalling that $||\bullet||_{\mathfrak{L}^2(\Gamma_D)} = \sqrt{\int_{\Gamma_D} \bullet^2 d\Gamma_D}$ is the $\mathfrak{L}^2(\Gamma_D)$-norm of function $\bullet$ along Γ_D. Once again, the resulting local error surfaces presented a similar general aspect, regardless of b degree, mesh or method, as exemplified for mesh 1, $b = 2$ on Figure 4.

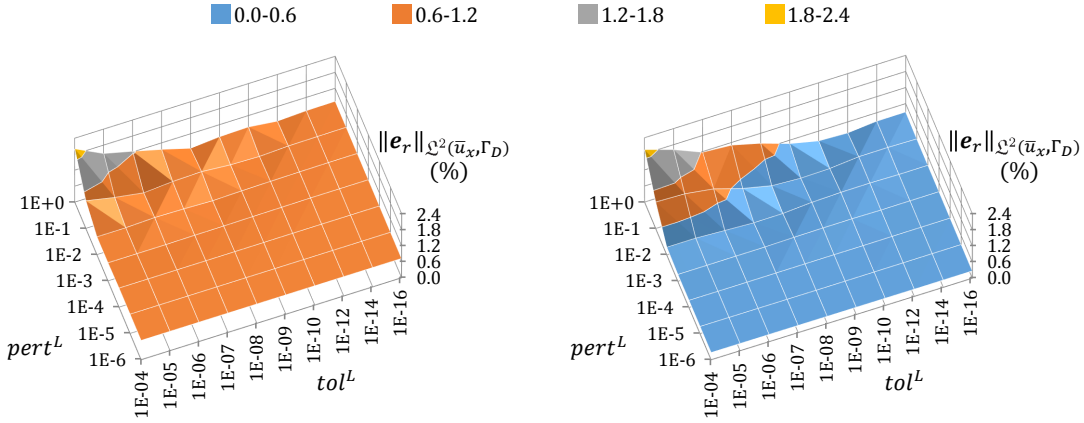

Figure 4: Local error surfaces for mesh 1 (Figure 2), $b = 2$ for different combinations of tolerance and perturbation the tolerance and perturbation to solve the local systems for the nodes on the Dirichlet boundary; Element-wise method (left) and Cloud-wise method (right).

The better approximation the cloud-wise method provides was noticeably clearer with these local analysis. With such study, it was possible to verify the values of each parameter which offers the best results, remarking that the results of this section were obtained using C^k-GFEM.

3.2 Global & Local Convergence

In the previous analysis, the relative error was considered in the form of energy norm. The purpose of using the energy norm and not simply the relative error is to be able to compare theoretical values presented by Szabó & Babuška (2011). Asymptotically, the error is approximated by

$$\log \|\boldsymbol{e}_r\|_E \approx \log C - \beta \log (DOF) \tag{21}$$

where the absolute value of β is the asymptotic convergence rate, DOF is the number of degrees of freedom and C is a constant problem dependent. The L-shaped domain problem falls into "category B" due to the presence of a singularity in the domain and hence, for conventional FEM, the following rate of convergence is known (Babuška & Suri, 1987):

- $\beta = \frac{1}{2}\min(b, \lambda_1)$ for h refinement; and
- $\beta = \min(\lambda_1, \frac{b}{2})$ for polynomial refinement;

recalling that λ_1, presented in the exact solution (16) and (17), indicates the degree of the singularity. After setting proper values for the perturbation factor ($pert^L = 10^{-0}$) and tolerance ($tol^L = 10^{-8}$) based on the study performed in section 3.1 regarding the solution of the local

systems, a conventional analysis for h and p refinement could be performed. The results are shown in Figure 5; in the legend, $M1$, $M2$, and $M3$ stand for meshes 1, 2, and 3 and C stands for the continuity of the PoU, classical C^0 or smooth C^k.

The term "free DOF" refers to the degrees of freedom (DOF) to which no coefficient is imposed, i.e., the total DOF minus the prescribed DOF. In the analysis, the number of free DOF was chosen to calculate the convergence rate in order to perform an appropriate comparison with the rates obtained by Babuška & Suri (1987) in their imposition of Neumann boundary conditions, for the internal elements (the ones without imposition of coefficients) are subjected to internal forces transmitted by the adjacent elements on the boundary, to which Dirichlet boundary conditions are imposed.

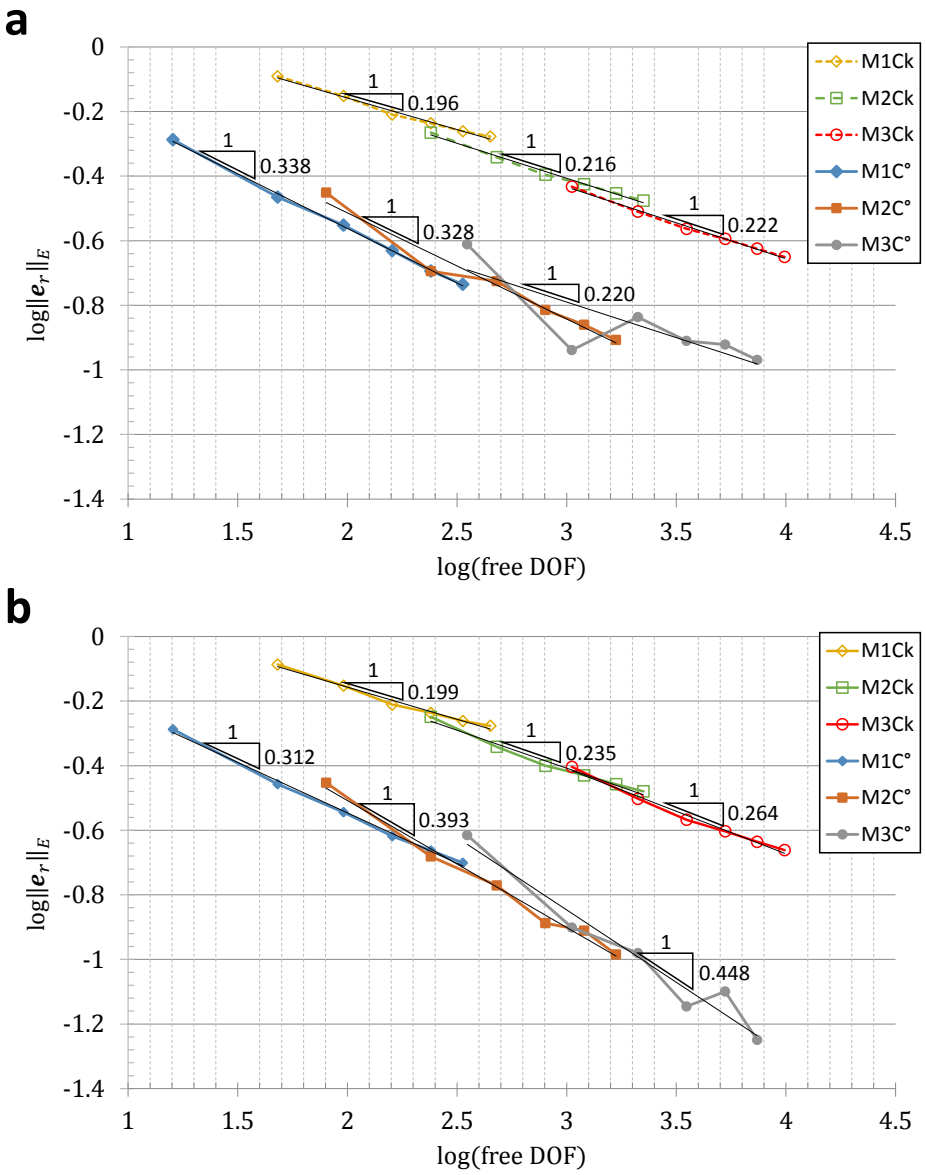

Figure 5: Convergence rate for meshes 1, 2, and 3 for polynomial refinement using $pert^L = 1$ and of $tol^L = 1 \times 10^{-8}$ in the local coefficients systems built by the cloud-wise method (a) and element-wise method (b).

As shown in Figure 5, the convergence rates obtained for the p refinement analysis are

below the expected theoretical asymptotic convergence rate for the conventional FEM, which, in this case, is $\lambda_1 = 0.544$ (except when $b = 1$, when $\beta = 0.5$), though it seems to approach this reference in the C^0-PoU element-wise case as the mesh is refined (Figure 5-b). However, the use of a C^0-PoU has shown to have caused oscillations in the results.

On the other hand, for the h refinement, the rates found in some cases were superior than theoretical values, while in others they were inferior, as shown in the Table 1. Also in this case, free DOF were used to calculate the convergence rate.

Table 1: Convergence rates for h-refinement using $pert^L = 1$ and of $tol^L = 1 \times 10^{-8}$ for solving the local coefficients systems.

	C^0		C^k	
b	Cloud-wise	Element-wise	Cloud-wise	Element-wise
1	0.241	0.244	0.254	0.236
2	0.353	0.331	0.267	0.261
3	0.213	0.325	0.263	0.266
4	0.209	0.393	0.267	0.273
5	0.170	0.326	0.271	0.279
6	0.175	0.408	0.278	0.287

Figures 6 and 7 present these results in a more visual manner, represented on the domain of the problem itself.

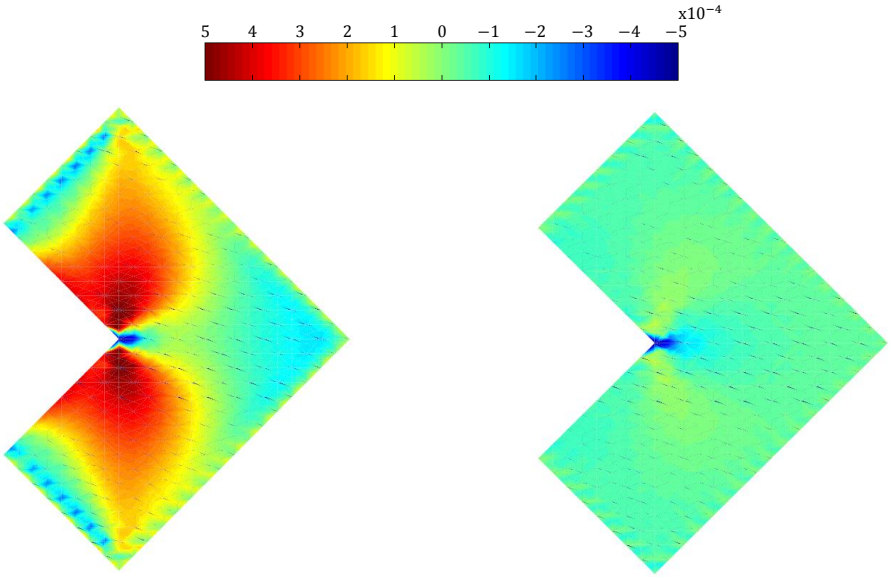

Figure 6: X-component of the exact error of the displacement comparing C^k PoU (left) and C^0 PoU (right) using the cloud-wise method, perturbation factor of 1 and tolerance of 1×10^{-8} in the local coefficients systems. Mesh 3 and $p = 2$.

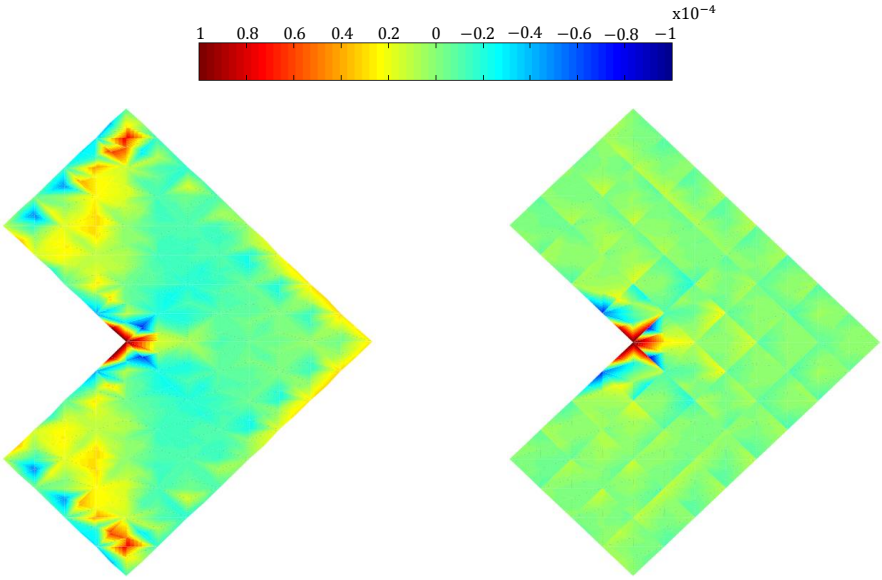

Figure 7: X-component of the exact error of the strain comparing C^k PoU (left) and C^0 PoU (right) using the cloud-wise method, perturbation factor of 1 and tolerance of 1×10^{-8} in the local coefficients systems. Mesh 2 and $p = 2$.

It is interesting to note how the use of the C^k PoU results in remarkably more errors on that portion of the boundary to which no nonhomogeneous Dirichlet boundary condition was prescribed (see Figure 2), and also how within the boundary elements, at the center of the elements, the error peaks inside of it. An analysis of the effects of the imposition of the coefficients in regards to the quality of the approximation on the elements close to the boundary and on those elements distant from the boundary is currently under study, as well as the rates at which the approximation at each portion improves its quality with respect to the continuity of the PoU, meshes, polynomial degree, and method of imposition of nonhomogeneous Dirichlet boundary conditions.

CONCLUDING REMARKS

The enforcement of nonhomogeneous Dirichlet boundary conditions in C^0 and C^k-GFEM using preprocessed nodal coefficients on the boundary was successfully imposed through the procedures explained throughout this work. Once the theory was understood, the construction of the linear systems to calculate coefficients was straightforward. Difficulties were encountered when solving the systems, but with aid of the least square method and experimentation with the approach proposed by Babuška et al. (2000), the coefficients could be computed.

It is remarked that in this early stage only continuously differentiable displacements are prescribed. One notice, however, that more general types of prescribed functions will require special enrichment functions at the boundary for representing special features. Two different manners of finding the node's coefficients have been proposed, and other different methods exist and deserve a further study and comparisons. A study regarding other different methods can be listed as a possible future work, as well as an analysis of the distribution of the error on the domain, as previously stated.

ACKNOWLEDGEMENTS

A. Rudnytskyj gratefully acknowledges the co-authors for the assistance in this work; special thanks to the professor D. A. F. Torres who relentlessly invested in the beginning, development and accomplishment of this work with remarkable guidance. The authors also acknowledge the financial support provided by CAPES (The Brazilian Federal Agency for Support and Evaluation of Graduate Education) and CNPq (The National Council for Scientific and Technological Development) at Brazil, during this research.

REFERENCES

Anderson, T. L., 2005. *Fracture Mechanics: fundamentals and applications*. 3th ed. CRC Press, Boca Raton, FL, USA.

Babuška, I. & Banerjee, U., 2012. Stable generalized finite element method (SGFEM). *Computer Methods in Applied Mechanics and Engineering*, vol. 201-204, p. 91-111.

Babuška, I., Caloz, G. & Osborn, J. E., 1994. Special finite element methods for a class of second order elliptic problems with rough coefficients. *SIAM Journal of Numerical Analysis*, vol. 31, p. 945-981.

Babuška, I. & Melenk, J. M., 1997. The partition of unity finite element method. *International Journal for Numerical Methods in Engineering*, vol. 40, p. 727-758.

Babuška, I. & Suri, M., 1987. The $h-p$ version of the finite element method with quasiuniform meshes. *ESAIM: Mathematical Modeling and Numerical Analysis - Modlisation Mathmatique et Analyse Numrique*, tome 21, n2, p. 199-238.

Babuška, I., Whiteman, J. R. & Strouboulis, T., 2011. *Finite elements: an introduction to the method and error estimation*. Oxford, New York.

de Barcellos, C. S., Mendonça, P. T. R. & Duarte, C. A., 2009. A C^k continuous generalized finite element formulations applied to laminated Kirchhoff plate model. *Computational Mechanics*, vol. 44, p. 377-393.

Barros, F. B., Proença, S. P. B., de Barcellos, C. S., 2004. On error estimator and p-adaptivity in the generalized finite element method. *International Journal for Numerical Methods in Engineering*, vol. 60, p. 23732398.

Béchet, E., Minnebo, H., Moës, N. & Burgardt, B., 2005. Improved implementation and robustness study of the XFEM for stress analysis around cracks. *International Journal for Numerical Methods in Engineering*, vol. 64, p. 1033-1056.

Belytschko. T. & Black, T., 1999. Elastic crack growth in finite elements with minimal remeshing. *International Journal for Numerical Methods in Engineering*, vol. 45, p. 601-620.

Belytschko, T., Gracie, R. & Ventura, G., 2009. A review of extended/generalized finite element methods for material modeling. *Modelling and Simulation in Material Science and Engineering*, vol. 17, paper 043001.

Cheney, E., Kincaid, D., 2007. *Numerical Mathematics and Computing*. 6th ed. Cengage Learning, Belmont, CA, USA.

Duarte, C. A., Babuška, I. & Oden, J. T., 2000. Generalized finite element method for three-dimensional structural mechanics problems. *Computers and Structures*, v. 77, p. 215-232.

Duarte, C. A., Kim, D. -J. & Quaresma, S. M., 2006. Arbitrarily smooth generalized finite element approximations. *Computer Methods in Applied Mechanics and Engineering*, vol. 196, p. 33-56.

Duarte, C. A. & Oden, J. T., 1995. *hp-Clouds: a meshless method to solve boundary-value problems*. Texas Institute for Computational and Applied Mathematics - The University of Texas at Austin. *Report*.

Duarte, C. A. & Oden, J. T., 1996. *hp-Clouds: a meshless method to solve boundary-value problems*. Texas Institute for Computational and Applied Mathematics - The University of Texas at Austin. *Report*.

Fries, T. -P. & Belytschko, T., 2006. The intrinsic XFEM: a method for arbitrary discontinuities without additional unknowns. *International Journal for Numerical Methods in Engineering*, vol. 68, p. 1358-1385.

Garcia, O. A., Fancello E. A., Mendonça, P. T. R., 2009. Developments in the application of the generalized finite element method to thick shell problems. *Computational Mechanics*, vol. 44, p. 669-682.

Gupta, V., Kim, D. -J., Duarte, C. A., 2012. Analysis and improvements of global-local enrichments for the generalized finite element method. *Computer Methods in Applied Mechanics and Engineering*, vol. 245-246, p. 47-62.

Mendonça, P. T. R., de Barcellos, C. S. & Torres, D. A. F., 2011. Analysis of anisotropic Mindlin plate model by continuous and non-continuous GFEM. *Finite Elements in Analysis and Design*, v. 47, p. 698-717.

Mendonça, P. T. R., de Barcellos, C. S. & Torres, D. A. F., 2013. Robust C^k/C^0 generalized FEM approximations for higher-order conformity requirements: application to Reddy's HSDT model for anisotropic laminated plates. *Composite Structures*, vol. 96, p. 332-345.

Melenk, J. M. & Babuška, I., 1996. The partition of unity finite element method: basic theory and applications. *Computer Methods in Applied Mechanics and Engineering*, vol. 139, p. 289-314.

Oden, J. T. & Reddy, J. N., 1976. *An introduction to the mathematical theory of finite elements*. John Wiley & Sons, New York, USA.

Rvachev, V. L. & Sheiko, T. I., 1995. R-functions in boundary value problems in mechanics. *Applied Mechanics Reviews*, vol. 48, p. 151-188.

Schaback, R., Wendland, H., 2006. Kernel techniques: from machine learning to meshless methods. *Acta Numerica*, vol. 15, p. 543-639.

Sillem, A., Simone, A., Sluys, L. J., 2015. The orthonormalized generalized finite element method (OGFEM): efficient and stable reduction of approximation errors through multiple orthonormalized enriched basis functions. *Computer Methods in Applied Mechanics and Engineering*, vol. 287, p. 112-149.

Strouboulis, T., Babuška, I., Copps, K., 2000. The design and analysis of the generalized finite

element method. *Computer Methods in Applied Mechanics and Engineering*, vol. 181, p. 43-69.

Strouboulis, T., Babuška, I., Copps, K., 2001. The generalized finite element method. *Computer Methods in Applied Mechanics and Engineering*, vol. 190, p. 4081-4193.

Szabó, B. A. & Babuška, I., 2011. *Introduction to finite element analysis: formulation, verification and validation*. John Wiley & Sons, Chichester, UK.

Torres, D. A. F., 2012. *Contribuições sobre a utilização de funções de aproximação contínuas no método generalizado de elementos finitos: avaliação em mecânica da fratura*. PhD thesis, Universidade Federal de Santa Catarina. In Portuguese.

Torres, D. A. F., Mendonça, P. T. R. & de Barcellos, C. S., 2011. Evaluation and verification of an HSDT-Layerwise generalized finite element formulation for adaptive piezoelectric laminated plates. *Computer Methods in Applied Mechanics and Engineering*, vol. 200, p. 675-691.

Torres, D. A. F., Mendonça, P. T. R. & de Barcellos, C. S., 2015. Effects of the smoothness of partitions of unity on the quality of representation of singular enrichments for GFEM/XFEM stress approximations around brittle cracks. *Computer Methods in Applied Mechanics and Engineering*, vol. 283, p. 243-279.

Wandzura, S. & Xiao, H., 2003. Symmetric quadrature rules on a triangle. *Computers and Mathematics with Applications*, vol. 45, p. 1829-1840.